DISCRETE AND CONTINUOUS
DYNAMICAL SYSTEMS SERIES B
Volume **24**, Number **6**, June **2019**

doi:10.3934/dcdsb.2018268

pp. **2639–2655**

BIFURCATION SCENARIOS IN AN ORDINARY DIFFERENTIAL EQUATION WITH CONSTANT AND DISTRIBUTED DELAY: A CASE STUDY

Tomás Caraballo

Departamento de Ecuaciones Diferenciales y Análisis Numérico
Universidad de Sevilla
c/ Tarfia s/n, 41012 Sevilla, Spain

Renato Colucci

Departament of Engineering,
University Niccolò Cusano
Via Don Carlo Gnocchi, 3 00166, Roma, Italy

Luca Guerrini

Department of Management, Polytechnic University of Marche
Piazza Martelli 8
60121, Ancona (AN), Italy

(Communicated by Xiaoying Han)

Abstract. In this article we consider a model introduced by Ucar in order to simply describe chaotic behaviour with a one dimensional ODE containing a constant delay. We study the bifurcation problem of the equilibria and we obtain an approximation of the periodic orbits generated by the Hopf bifurcation. Moreover, we propose and analyse a more general model containing distributed time delay. Finally, we propose some ideas for further study. All the theoretical results are supported and illustrated by numerical simulations.

1. **Introduction.** In [18] the author introduced a simple model to describe chaotic behaviour. The proposed system is unidimensional, contains time delay and presents a simple nonlinear cubic term:

$$\dot{x}(t) = \delta x(t-\tau) - \varepsilon \left[x(t-\tau)\right]^3, \tag{1}$$

where δ and ε are positive parameters and τ is a time delay. By means of some numerical experiments the author illustrates in [18] the rich behaviour of the system (see also [19]).

The model has attracted the interest of researchers (see for example [1] in which a fractional order version of the system is considered).

2010 *Mathematics Subject Classification.* 35B32, 74H65, 34K60.

Key words and phrases. Differential equation with delay, Hopf bifurcation, qualitative behaviour of solutions, distributed time delay.

This work has been partially supported by FEDER and the Spanish Ministerio de Economía y Competitividad project MTM2015-63723-P and the Consejería de Innovación, Ciencia y Empresa (Junta de Andalucía) under grant 2010/FQM314 and Proyecto de Excelencia P12-FQM-1492.

The rigorous mathematical analysis of the model has been carried out in [8], where the authors applied the normal form theory and the center manifold theorem to investigate the stability and direction of the bifurcating periodic orbits for equation (1), providing also numerical examples to support the theoretical analysis.

Other rigorous results have been obtained in [2], where, using critical curves approach, the authors study the problem of bifurcation with respect to the time delay parameter. Furthermore, a model with two different constant delays has been proposed and partially analysed in [3] (see also [9, 10, 11] for other models with delays).

In this paper we reconsider the Hopf bifurcation analysis (see section 2 below) obtaining slightly different results with respect to those proved in [8]. Moreover, using a different approach, namely applying the perturbation method known as the Lindstedt expansion (see e.g. [17]), we perfom a detailed analysis of the problem of approximation of the bifurcating periodic solutions (see Section 3).

Next, we introduce a generalised version of the model by considering distributed time delay for which stability and bifurcation analysis is carried out in Section 4. We will highlight that distributed delays appear to regularise the dynamics, in fact only fixed points or periodic orbits are in the attractor of the system.

In Section 5 we provide several numerical simulations to illustrate the theoretical results. Finally, Section 6 is devoted to state some conclusive remarks and propose further studies about this topic.

2. Stability and Hopf bifurcation analysis for the model with constant delay.

In this section, local stability of the equilibrium points is investigated. Equation (1) possesses three equilibrium points x_*, which are obtained solving the equality:

$$\delta x_* - \varepsilon x_*^3 = 0.$$

In other words, $x_* = 0, \pm\sqrt{\delta/\varepsilon}$.

The linearisation of equation (1) at x_* is given by

$$\dot{x} = a\left[x(t-\tau) - x_*\right],$$

where

$$a = \delta - 3\varepsilon x_*^2.$$

We have $a = \delta$ if $x_* = 0$ and $a = -2\delta$ if $x_* = \pm\sqrt{\delta/\varepsilon}$, and the associated characteristic equation is

$$\lambda - ae^{-\lambda\tau} = 0. \tag{2}$$

Obviously, when $\tau = 0$, the equilibria $x_* = \pm\sqrt{\delta/\varepsilon}$ are locally asymptotically stable, while the equilibrium $x_* = 0$ is unstable.

As τ increases, the stability properties may change if (2) possesses zero or a pair of purely imaginary eigenvalues. It is straightforward that the case $\lambda = 0$ cannot occur.

Lemma 1. *Eq. (2) possesses a pair of purely imaginary roots $\lambda = \pm i\omega_*$ at the critical value $\tau = \tau_*$, where $\omega_* = \delta$ and $\tau_* = 3\pi/(2\delta)$ if $x_* = 0$, and $\omega_* = 2\delta$ and $\tau_* = \pi/(4\delta)$ if $x_* = \pm\sqrt{\delta/\varepsilon}$.*

Proof. Suppose that $\lambda = i\omega$ (with $\omega > 0$) is a root of (2). Then, ω satisfies $i\omega = ae^{-i\omega\tau}$. Separating the real and imaginary parts of the equality,

$$\omega = -a\sin\omega\tau, \quad 0 = a\cos\omega\tau. \tag{3}$$

Eliminating τ from (3),

$$\omega^2 = a^2, \text{ i.e. } \omega = |a|.$$

Notice that, if $x_* = 0$, then (3) becomes

$$\omega = -\delta \sin \omega\tau, \qquad 0 = \cos \omega\tau.$$

Since $\omega > 0$, we must have $\sin \omega\tau < 0$. Thus, $\omega\tau = 3\pi/2$.

On the other hand, if $x_* = \pm\sqrt{\delta/\varepsilon}$, then equations in (3) take the form

$$\omega = 2\delta \sin \omega\tau, \qquad 0 = \cos \omega\tau.$$

Since $\sin \omega\tau > 0$ we obtain that $\omega\tau = \pi/2$. Notice that $\lambda = i\omega_*$ is a simple root of (2). Indeed, if it were a multiple root, then $1 + a\tau_* e^{i\omega_*\tau_*} = 0$, i.e. $1 + a\tau_* \cos \omega_*\tau_* = 0$ and $-a\tau_* \sin \omega_*\tau_* = 0$. From (3) we obtain a contradiction. □

We now analyse the direction of the bifurcation.

Theorem 2. *Let τ_* be defined as in the previous Lemma.*

1. *The equilibrium $x_* = 0$ of (1) is unstable for all $\tau \geq 0$.*
2. *The equilibria $x_* = \pm\sqrt{\delta/\varepsilon}$ of (1) are locally asymptotically stable for $\tau \in [0, \tau_*)$ and unstable for $\tau > \tau_*$. Furthermore, (1) undergoes a Hopf bifurcation at x_* when $\tau = \tau_*$.*

Proof. For simplicity we set $\lambda(\tau) = \alpha(\tau) + i\omega(\tau)$, that is a root of (2) satisfying $\alpha(\tau_*) = 0$ and $\omega(\tau_*) = \omega_*$. Differentiating the characteristic equation (2) with respect τ, we obtain

$$\frac{d\lambda}{d\tau} = -\frac{\lambda^2}{1 + \tau\lambda},$$

and, consequently,

$$sign\left\{\frac{d\,(Re\lambda)}{d\tau}\bigg|_{\tau=\tau_*}\right\} = sign\left\{\frac{\omega_*^2}{1 + \tau_*^2\omega_*^2}\right\}.$$

Thus, we conclude that

$$\frac{d\,(Re\lambda)}{d\tau}\bigg|_{\tau=\tau_*} > 0.$$

The previous inequality implies that the roots $\lambda = \pm i\omega_*$ of the characteristic equation (2) near τ_* crosses the imaginary axis from the left to the right as τ continuously varies from a number less than τ_* to one greater than τ_*. □

Remark 3. As previously observed in the literature, the critical value of the parameter chosen for the bifurcation analysis only depends on δ and it is independent of ε.

2.1. **Numerical simulations.** For simplicity we set

$$P_- := -\sqrt{\frac{\delta}{\varepsilon}}, \qquad P_+ := \sqrt{\frac{\delta}{\varepsilon}},$$

We fix the values of the parameters as follows

$$\varepsilon = \delta = 1,$$

from which we obtain that

$$P_- = -1, \quad P_+ = 1, \quad \tau_* \approx 0.785398.$$

In the first numerical experiment (see figure 1) we fix $\tau = 0.7 < \tau_*$ and solutions starting in the positive semiaxes converge to P_+, while the ones starting in the negative semiaxes converge to P_-.

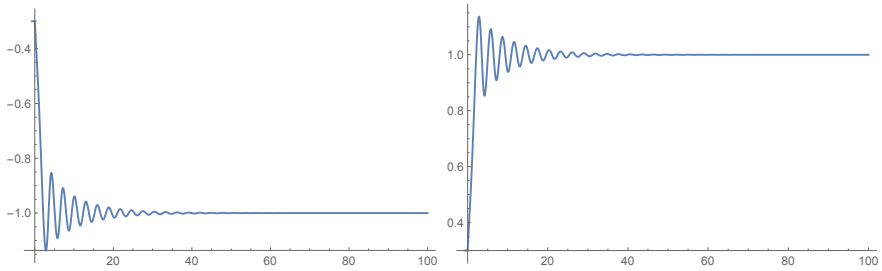

FIGURE 1. The solution starting on the left hand side of O converges to $P_- = -1$, while that starting on the right hand side of O converges to $P_+ = 1$.

In the second numerical experiment (see figure 2) we fix $\tau = 0.8 > \tau_*$, all the fixed points are unstable, two stable limit cycles appear around P_- and P_+.

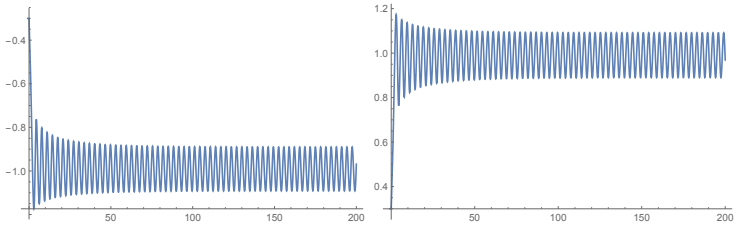

FIGURE 2. The solution starting on the left hand side of O converges to a limit cycle around P_-, while that starting on the right hand side of O converges to a limit cycle around P_+.

If we increase the value of τ we observe a more complex behaviour. In figure 3 we represent the solution when $\tau = 1.72$, where the dynamical behaviour of solutions appear to be chaotic.

3. Approximating expressions of the bifurcating periodic solutions.

In this section we consider the problem of approximating the periodic orbits generated by the Hopf Bifurcation. For this purpose we use the perturbation method known as the Lindstedt expansion. Thanks to the approximated periodic solutions we will be able to determine the direction of the Hopf bifurcation and the period of the bifurcating periodic solution. Our main result is the following:

Theorem 4. *The Hopf bifurcation of Eq. (1) at the equilibrium point $x_* = \pm\sqrt{\delta/\varepsilon}$ when $\tau = \tau_*$ is supercritical and the bifurcating periodic solutions exist for $\tau > \tau_*$. In addition, its period increases as τ increases.*

Proof. We split the proof into two parts.
Step 1. *Construction of the approximation*

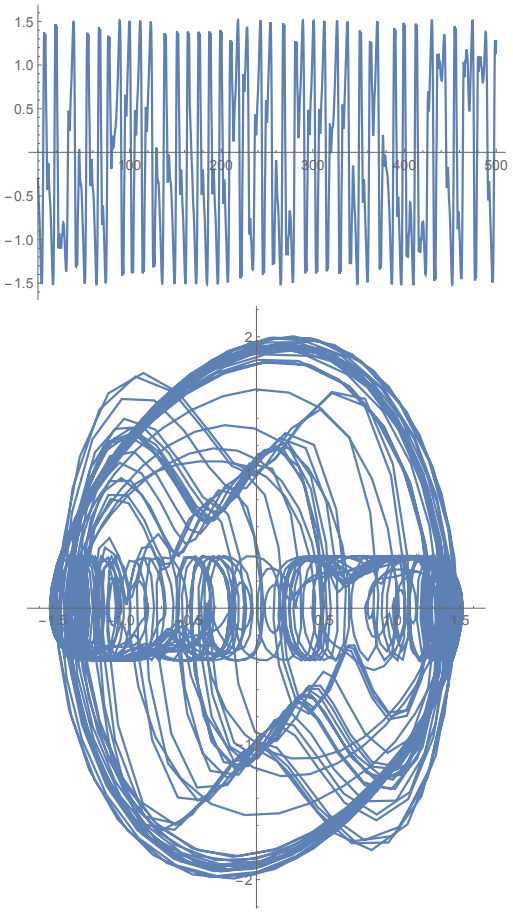

FIGURE 3. The solution $x(t)$ and the graph of $(x(t), x'(t))$ for $\delta = \varepsilon = 1$ and $\tau = 1.72$. The attractor appears to be chaotic.

First of all we consider the change of variable $z = x - x_*$ in equation (1), where $x_* = \pm\sqrt{\delta/\varepsilon}$. Then we take the Taylor expansion of the resulting equation at $z = 0$:

$$\dot{z} = a_1 z(t-\tau) + a_2 z(t-\tau)^2 + a_3 z(t-\tau)^3 + \cdots, \tag{4}$$

where

$$a_1 = -2\varepsilon x_*^2, \qquad a_2 = -6\varepsilon x_*, \qquad a_3 = -6\varepsilon.$$

To apply Poincaré-Lindstedt perturbation method we stretch time with the transformation $s = \omega(\eta)t$, where η is a small positive number so that solutions which are $2\pi/\omega$ periodic in t become 2π periodic in s. Hence, (4) can be rewritten as follows:

$$\omega \frac{dz(s)}{ds} = a_1 z\left(s - \omega\tau\right) + a_2 z\left(s - \omega\tau\right)^2 + a_3 z\left(s - \omega\tau\right)^3 + \cdots. \tag{5}$$

Next, we expand the solution of (5) in power series of η:

$$z(s) = z_0(s)\eta + z_1(s)\eta^2 + z_2(s)\eta^3 + \cdots, \tag{6}$$

and we solve it for the unknown functions $z_j(s)$ recursively, i.e., in the order $z_0(s), z_1(s)$,...

Moreover, we expand the frequency ω and the delay τ in powers of η in a similar way

$$\omega = \omega(\eta) = \omega_0 + \omega_1\eta + \omega_2\eta^2 + \cdots, \quad \tau = \tau(\eta) = T_0 + T_1\eta + T_2\eta^2 + \cdots, \tag{7}$$

where

$$T_0 = \tau_* = \pi/(4\delta), \quad \text{and} \quad \omega_0 = \omega_* = 2\delta.$$

From (6) and (7), we obtain the following expression for $z(s-\omega\tau)$:

$$z(s-\omega\tau) = z_0(s-\omega\tau)\eta + z_1(s-\omega\tau)\eta^2 + z_2(s-\omega\tau)\eta^3 + \cdots \tag{8}$$

In details, the expression of $z_j(s-\omega\tau)$ is

$$\begin{aligned} z_j(s-\omega\tau) &= z_j(s-\omega_0T_0) \\ &\quad - z_j'(s-\omega_0T_0)\left[(\omega_1T_0+\omega_0T_1)\eta + (\omega_2T_0+\omega_1T_1+\omega_0T_2)\eta^2 + \cdots\right] \\ &\quad + \frac{1}{2}z_j''(s-\omega_0T_0)\left[(\omega_1T_0+\omega_0T_1)\eta + \cdots\right]^2 - \cdots, \end{aligned}$$

with the prime denoting differentiation with respect to s. Plugging (6), (7) and (8) into (5), and matching the coefficients of the various terms involving powers of η (till the third order) we obtain the following equations:

$$O(\eta): \quad \omega_0\frac{dz_0(s)}{ds} = a_1 z_0(s-\omega_0T_0), \tag{9}$$

$$\begin{aligned} O(\eta^2): \quad \omega_0\frac{dz_1(s)}{ds} + \omega_1\frac{dz_0(s)}{ds} &= -a_1z_0'(s-\omega_0T_0)(\omega_1T_0+\omega_0T_1) \\ &\quad + a_1z_1(s-\omega_0T_0) + a_2z_0^2(s-\omega_0\tau_0), \end{aligned} \tag{10}$$

$$\begin{aligned} O(\eta^3): \quad &\omega_0\frac{dz_2(s)}{ds} + \omega_1\frac{dz_1(s)}{ds} + \omega_2\frac{dz_0(s)}{ds} \\ &\quad = -a_1z_0'(s-\omega_0T_0)(\omega_2T_0+\omega_1T_1+\omega_0T_2) \\ &\quad + 2a_2z_0(s-\omega_0T_0)z_1(s-\omega_0T_0) + \frac{1}{2}a_1z_0''(s-\omega_0T_0)(\omega_1T_0+\omega_0T_1)^2 \\ &\quad + a_1z_2(s-\omega_0T_0) - a_1z_1'(s-\omega_0T_0)(\omega_1T_0+\omega_0T_1) + a_3z_0(s-\omega_0T_0)^3. \end{aligned} \tag{11}$$

The general solution of equation (9) is

$$z_0(s) = A_0\sin s + B_0\cos s, \tag{12}$$

where A_0 and B_0 are constants to be determined. Substituting (12) into (9), we derive that A_0 and B_0 are arbitrary. Without loss of generality, we suppose that the initial conditions are $z_0(0) = 0$ and $z_0'(0) = 1$. As a result, (12) becomes

$$z_0(s) = \sin s. \tag{13}$$

Next, we look for a solution of equation (10) of the following form

$$z_1(s) = A_1\sin s + B_1\cos s + C_1\sin 2s + D_1\cos 2s + E_1, \tag{14}$$

where coefficients A_1, B_1, C_1, D_1 and E_1 are constant. Replacing the expression of $z_0(s)$ from (13) and that of $z_1(s)$ from (14) into (10), recalling $\omega_0T_0 = \pi/2$, and

based on trigonometric functions properties, we obtain

$$\omega_0\left(A_1\cos s - B_1\sin s + 2C_1\cos 2s - 2D_1\sin 2s\right) + \omega_1\cos s$$
$$= -a_1(\omega_1 T_0 + \omega_0 T_1)\sin s$$
$$+ a_1\left(-A_1\cos s + B_1\sin s - C_1\sin 2s - D_1\cos 2s + E_1\right) + \frac{a_2}{2} + \frac{a_2}{2}\cos 2s.$$

Equating the coefficients of the resonant terms $\sin s, \cos s, \sin 2s$ and $\cos 2s$, and recalling that $\omega_0 = -a_1$, yield

$$\omega_1 = T_1 = 0, \qquad C_1 = -\frac{a_2}{5a_1}, \qquad D_1 = \frac{a_2}{10a_1}, \qquad E_1 = -\frac{a_2}{2a_1}, \tag{15}$$

with A_1 and B_1 arbitrary. Letting, for simplicity, $A_1 = B_1 = 0$, it follows that (14) reduces to

$$z_1(s) = C_1\sin 2s + D_1\cos 2s + E_1, \tag{16}$$

where C_1, D_1 and E_1 are given in (15). Since $\omega_1 = T_1 = 0$, we have that (11) can be rewritten as

$$\omega_0\frac{dz_2(s)}{ds} + \omega_2\frac{dz_0(s)}{ds} = -a_1 z_0'(s-\omega_0 T_0)(\omega_2 T_0 + \omega_0 T_2) + a_1 z_2(s-\omega_0 T_0)$$
$$+ 2a_2 z_0(s-\omega_0 T_0)z_1(s-\omega_0 T_0) + a_3 z_0(s-\omega_0 T_0)^3. \tag{17}$$

Let

$$z_2(s) = A_2\sin s + B_2\cos s + C_2\sin 2s + D_2\cos 2s + E_2\sin 3s + F_2\cos 3s + G_2 \tag{18}$$

be solution of (17), with $A_2, B_2, C_2, D_2, E_2, F_2$ and G_2 constants. Using (13),(16) and (18) in (17), after trigonometric simplifications have been performed, by comparing the coefficients of the terms $\sin s, \cos s, \sin 2s, \cos 2s, \sin 3s$ and $\cos 2s$, we obtain the following expressions

$$\omega_2 = \frac{a_2^2}{a_1} = -18\varepsilon^2 \quad \text{and} \quad \tau_2 = -\frac{\pi a_2^2}{2a_1^3} = \frac{9\pi}{4\varepsilon x_*^4}. \tag{19}$$

Summing up all the above analysis, the bifurcated periodic solution of (1) has the approximated form

$$z(s) = \sqrt{\frac{\tau - T_0}{T_2}}z_0(s) + \frac{\tau - T_0}{T_2}z_1(s) + \cdots, \tag{20}$$

where $z_0(s), z_1(s)$ are given in (13) and (16) respectively, and $\tau \approx T_0 + T_2\eta^2$, $\omega \approx \omega_0 + \omega_2\eta^2$.

Step 2. *Analysis of the bifurcation*

The parameters τ_2 and ω_2 determine the direction of the Hopf bifurcation and the period of the bifurcating periodic solution, respectively. Since $\omega_2 < 0$ and $\tau_2 > 0$, we obtain the thesis of our theorem. □

3.1. **Numerical simulations.** Let us fix the parameters as in the previous section:

$$\varepsilon = \delta = 1.$$

We choose $\tau = 0.8 > \tau_*$, in figure 4 we represent the numerical solution in red together with its approximation (in blue). We observe that the periods are the same, while the amplitude of the approximated solution is lower than that of the numerical solution. This, of course, is due to the missing terms z_i with $i \geq 2$.

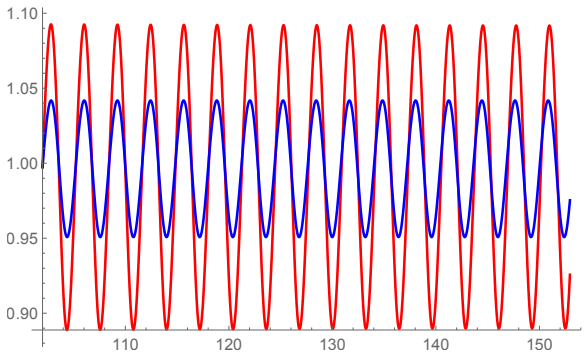

FIGURE 4. The numerical solution (in red) together with its approximation (in blue) given by (20).

4. **Model with distributed delays.** In the last decades, the effects of distributed delay in complex system have attracted the interests of many researchers (see for example [13], [5])

For this reason, we consider interesting to modify equation (1) by introducing a distributed delay as follows

$$\dot{x}(t) = \delta \int_{-\infty}^{t} x(r)g(t-r)dr - \varepsilon \left[\int_{-\infty}^{t} x(r)g(t-r)dr \right]^3, \tag{21}$$

where $g(\cdot)$ is a gamma distribution of the kind:

$$g(u) = \left(\frac{m}{T}\right)^m \frac{u^{m-1}e^{-\frac{m}{T}u}}{(m-1)!}, \tag{22}$$

with m a positive integer that determines the shape of the weighting function, and $T \geq 0$ a parameter associated with the mean time delay of the distribution.

For $m = 1$ this is simply an exponential distribution (also called a weak delay kernel); for $m = 2$ it is known as strong delay kernel. Notice that as $T \to 0$ the distribution function approaches the Dirac distribution, and, thus, one recovers the discrete delay case.

We set $z(t) = x(t) - x_*$, where x_* is a stable equilibrium point of equation (1), i.e. $x_* = \pm\sqrt{\delta/\varepsilon}$.

The linearised equation of (21) at the origin takes the form

$$\dot{z}(t) = -2\delta \int_{-\infty}^{t} z(r)g(t-r)dr. \tag{23}$$

In equation (23), we make the ansatz that $z(t) = ce^{\lambda t}$, $c \in \mathbb{R}$, $\lambda \in \mathbb{C}$, to obtain the associated characteristic equation

$$\lambda + 2\delta \int_{-\infty}^{t} e^{-\lambda(t-r)}g(t-r)dr = 0. \tag{24}$$

By mathematical induction we have

$$\int_{-\infty}^{t} e^{-\lambda(t-r)} g(t-r)dr = \int_{0}^{+\infty} e^{-\lambda v} g(v)dv$$

$$= \left(\frac{m}{T}\right)^m \frac{1}{(m-1)!} \int_{0}^{+\infty} v^{m-1} e^{-\left(\frac{m}{T}+\lambda\right)v} dv = \left(1+\frac{\lambda T}{m}\right)^{-m}.$$

As a consequence, the characteristic equation (24) becomes

$$\lambda\left(1+\frac{\lambda T}{m}\right)^m + 2\delta = 0. \tag{25}$$

Since $\lambda = 0$ is not a solution of this equation, the only possibility for the stability of $z_* = 0$ to change is that λ crosses the imaginary axis.
Equation (25) is a polynomial equation of degree $n = m + 1$ which possesses the form

$$\lambda^n + a_1\lambda^{n-1} + \cdots + a_{n-1}\lambda + a_n = 0, \tag{26}$$

where coefficients a_k are real constants. Then, the Routh-Hurwitz theorem provides the necessary and sufficient conditions for all the roots of the polynomial equation (26) to have negative real parts. To apply this theorem, we first construct the $n \times n$ Routh-Hurwitz matrix

$$\begin{bmatrix} a_1 & 1 & 0 & 0 & \cdots & 0 \\ a_3 & a_2 & a_1 & 1 & \cdots & 0 \\ a_5 & a_4 & a_3 & a_2 & \cdots & 0 \\ \vdots & \vdots & \vdots & \vdots & \cdots & \vdots \\ 0 & 0 & 0 & 0 & \cdots & a_n \end{bmatrix},$$

where $a_k = 0$ for $k > n$. The Routh-Hurwitz criterion states that all roots of equation (26) are negative or have negative real part if and only if all the principal minors Δ_k $(k = 0, 1, 2, ..., n)$ of the Routh-Hurwitz matrix are positive.

When $n = 2$, that is $m = 1$, we have

$$\lambda^2 + a_1\lambda + a_2 = 0,$$

and the criteria simplify to

$$a_1 > 0, \quad \text{and} \quad a_2 > 0.$$

For $n = 3$, that is $m = 2$, the characteristic polynomial is

$$\lambda^3 + a_1\lambda^2 + a_2\lambda + a_3 = 0,$$

and the criteria become

$$a_1 > 0, \quad a_3 > 0, \quad \text{and} \quad a_1a_2 > a_3.$$

Finally, for $n = 4$, that is $m = 3$, we have the polynomial

$$\lambda^4 + a_1\lambda^3 + a_2\lambda^2 + a_3\lambda + a_4 = 0,$$

and the criteria are

$$a_1 > 0, \quad a_3 > 0, \quad a_4 > 0 \quad \text{and} \quad a_1a_2a_3 > a_3^2 + a_1^2a_4.$$

Notice that a direct consequence of the Routh-Hurwitz theorem is that all the coefficients are positive, $a_k > 0$ $(k = 1, 2, ..., n)$.

In order to analytically consider local stability of our equilibrium we will consider several special cases separately.

4.1. **Case** $m = 1$**.** Equation (25) reduces to a second order algebraic equation in λ, $\lambda^2 + a_1\lambda + a_2 = 0$, where $a_1 = 1/T$ and $a_2 = 2\delta/T$. Due to the Routh-Hurwitz criterion we have the following result.

Proposition 5. *The equilibrium points* $x_* = \pm\sqrt{\delta/\varepsilon}$ *of* (21)*are locally asymptotically stable for all* $T > 0$.

4.2. **Case** $m = 2$**.** Equation (25) takes the form of a third order algebraic equation in λ,

$$\lambda^3 + a_1\lambda^2 + a_2\lambda + a_3 = 0, \tag{27}$$

where

$$a_1 = a_1(T) = 4/T, a_2 = a_2(T) = 4/T^2 \quad a_3 = a_3(T) = 8\delta/T^2.$$

The Routh-Hurwitz criterion implies that the equilibria $x_* = \pm\sqrt{\delta/\varepsilon}$ are locally asymptotically stable if $a_1a_2 - a_3 = 8T\,(2 - \delta T) > 0$, i.e. $T < 2/\delta$, and unstable if $T > 2/\delta$. The curve $T = T_* = 2/\delta$ divides the parameter space into stable and unstable parts. To check the possibility of the emergency of a limit cycle at $T = T_*$, we apply the Hopf bifurcation theorem. According to it, one can establish the existence of a cyclic solution if the characteristic equation (27) possesses a pair of purely imaginary roots and the real parts of these roots change signs with a bifurcation parameter.

At the critical value $T = T_*$, the characteristic equation (27) can be written as $\lambda^3 + a_1(T_*)\lambda^2 + a_2(T_*)\lambda + a_1(T_*)a_2(T_*) = 0$, which factorises as

$$[\lambda + a_1(T_*)]\left[\lambda^2 + a_2(T_*)\right] = 0.$$

Hence, we have a pair of purely imaginary roots $\lambda_{1,2} = \pm\sqrt{a_2(T_*)}i = \pm\omega_* i$, with $\omega_* = \delta$, and a real root $\lambda_3 = -a_1 = -2\delta$. Next, we choose the delay T as the bifurcation parameter and consider the roots of the characteristic equation (27) as continuous functions of T. Plugging $\lambda = \lambda(T)$ into (25), with $m = 2$, and differentiating it with respect to T implies

$$\frac{d\lambda}{dT} = -\frac{2\lambda^2}{2 + 3T\lambda}. \tag{28}$$

Notice the rootof (27), $\lambda = \omega_* i$, is simple. Next, replacing $\lambda = \omega_* i$ into (28), and rationalizing the right hand side conduced us to

$$Re\left[\frac{d\lambda}{dT}\right]_{\lambda=\omega_* i} = \frac{4\omega_*^2}{4 + 9T^2\omega_*^2} > 0.$$

As a result, the real parts of the complex roots change from being negative to positive and, therefore, there is a loss of stability on the partition curve. The above analysis can be summarised as follows.

Theorem 6. *Let* $T_* = 2/\delta$*. The equilibrium points* $x_* = \pm\sqrt{\delta/\varepsilon}$ *of* (21) *are locally asymptotically stable for* $T < T_*$ *and unstable for* $T > T_*$*. System* (21) *undergoes a Hopf bifurcation at* x_* *when* $T = T_*$.

4.3. **Case** $m = 3$**.** Equation (25) becomes a fourth order algebraic equation in λ,

$$\lambda^4 + a_1\lambda^3 + a_2\lambda^2 + a_3\lambda + a_4 = 0, \tag{29}$$

where

$$a_1 = a_1(T) = 9/T, a_2 = a_2(T) = 27/T^2, a_3 = a_3(T) = 27/T^3,$$
$$\text{and} \quad a_4 = a_4(T) = 54\delta/T^3.$$

By the Routh-Hurwitz criterion, the equilibria $x_* = \pm\sqrt{\delta/\varepsilon}$ are locally asymptotically stable if $a_1a_2a_3 - a_3^2 + a_1^2a_4 > 0$. A direct calculation shows this holds when $T < T_* = 4/(3\delta)$. At the critical value $T = T_*$, i.e. when

$$a_1a_2a_3 - a_3^2 + a_1^2a_4 = 0,$$

the characteristic equation (29) factorises as

$$\left[a_1(T_*)\lambda^2 + a_3(T_*)\right]\left[a_1(T_*)\lambda^2 + a_1^2(T_*)\lambda + a_1(T_*)a_2(T_*) - a_3(T_*)\right] = 0.$$

Its solutions are $\lambda_{1,2} = \pm\sqrt{-a_3(T_*)/a_1(T_*)} = \pm\left(3/T_*^2\right)i$, which are purely imaginary, and $\lambda_{3,4} = 3\delta\left(-9 \pm \sqrt{15}i\right)/8$, whose real parts are negative. Proceeding as for $m = 1$, we derive that

$$\frac{d\lambda}{dT} = -\frac{3\lambda^2}{3 + 4T\lambda},$$

and hence

$$Re\left[\frac{d\lambda}{dT}\right]_{\lambda=\omega_* i} = \frac{9\omega_*^2}{9 + 16T^2\omega_*^2} > 0.$$

Consequently, the dynamical system generates cyclic behaviour when the local stability is violated. We summarise the previous discussion in the following theorem.

Theorem 7. *Let $T_* = 4/(3\delta)$. The equilibrium points $x_* = \pm\sqrt{\delta/\varepsilon}$ of (21) are locally asymptotically stable for $T < T_*$ and unstable for $T > T_*$. System (21) undergoes a Hopf bifurcation at x_* when $T = T_*$.*

5. **Numerical simulations for the model with distributed delay.** In order to numerically analyse the stability switch and global behaviour of the equilibrium x_*, we apply the linear chain trick technique (see [12]) which allows to replace an equation with the gamma distributed delay kernel (22) by an equivalent system of $(m + 1)$ ordinary differential equations.

5.1. **Case** $m = 1$**.** Equation (21) becomes

$$\dot{x}(t) = \delta \int_{-\infty}^{t} x(r)\left(\frac{1}{T}\right)e^{-\frac{1}{T}u}dr - \varepsilon\left[\int_{-\infty}^{t} x(r)\left(\frac{1}{T}\right)e^{-\frac{1}{T}u}dr\right]^3. \tag{30}$$

Introducing the new variable

$$y(t) = \int_{-\infty}^{t} x(r)\left(\frac{1}{T}\right)e^{-\frac{1}{T}(t-r)}dr,$$

we rewrite equation (30) as a two dimensional system of ODEs:

$$\begin{cases} \dot{x}(t) &= \delta y(t) - \varepsilon y(t)^3, \\ \dot{y}(t) &= \dfrac{1}{T}\left[x(t) - y(t)\right]. \end{cases}$$

We consider the following values of the parameters for the simulations:

$$\delta = 1, \quad \varepsilon = 1, \quad T = 30.$$

The fixed points are $P_+ = (1,1)$, $O = (0,0)$ and $P_- = (-1,-1)$. From the result of the previous sections, the fixed points $P_\pm$ remain locally asymptotically stable for all $T \geq 0$ (see figure 5).

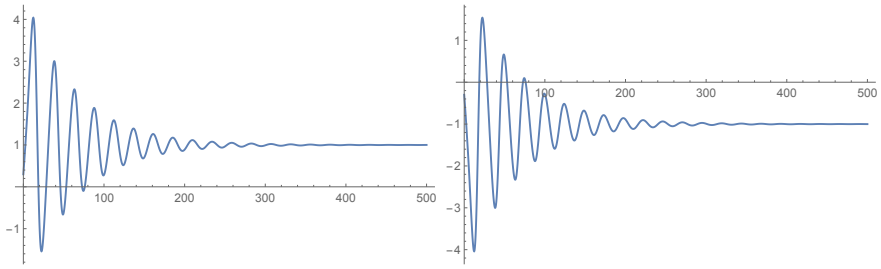

FIGURE 5. For $m = 1$, the fixed points $P_\pm$ are locally asymptotically stable for all $T \geq 0$.

5.2. **Case $m = 2$.** Equation (21) becomes

$$\dot{x}(t) = \delta \int_{-\infty}^{t} x(r) \left(\frac{2}{T}\right) (t-r) e^{-\frac{2}{T}(t-r)} dr - \varepsilon \left[\int_{-\infty}^{t} x(r) \left(\frac{2}{T}\right)^2 (t-r) e^{-\frac{2}{T}(t-r)} dr \right]^3. \tag{31}$$

Introducing the new variables

$$y(t) = \int_{-\infty}^{t} x(r) \left(\frac{2}{T}\right)^2 (t-r) e^{-\frac{2}{T}(t-r)} dr,$$

$$z(t) = \int_{-\infty}^{t} x(r) \left(\frac{2}{T}\right) e^{-\frac{2}{T}(t-r)} dr,$$

we rewrite equation (31) as a three dimensional system of ODEs:

$$\begin{cases} \dot{x}(t) &= \delta y(t) - \varepsilon y(t)^3, \\ \dot{y}(t) &= \dfrac{2}{T}\left[z(t) - y(t)\right], \\ \dot{z}(t) &= \dfrac{2}{T}\left[x(t) - z(t)\right]. \end{cases}$$

In this case we have shown that for $T < T_*$ the fixed point $P_\pm$ are locally asymptotically stable while for $T = T_*$ a Hopf bifurcation occurs at $P_\pm$ giving rise to stable limit cycles.

We consider the following values of the parameters:

$$\delta = 2, \quad \varepsilon = 1,$$

from which we obtain the following numerical values for the fixed points $P_\pm$ and for the critical value of T:

$$T_* = 1, \qquad P_\pm = \pm(\sqrt{2}, \sqrt{2}, \sqrt{2}).$$

In a first simulation we have set $T = 0.9 < T_*$ for which the fixed points $P_\pm$ are locally asymptotically stable (see figure 6).

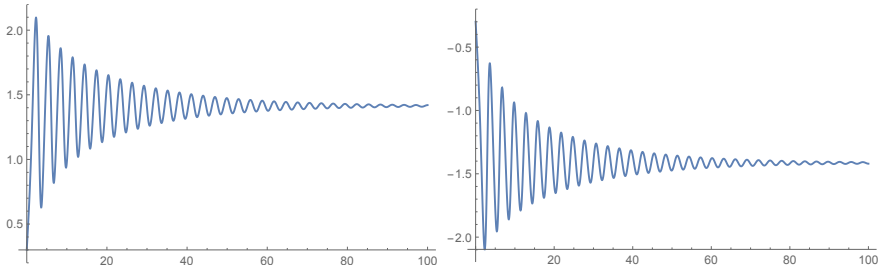

FIGURE 6. For m=2 and $T = 0.9 < T_*$ the fixed points $P_\pm$ are locally asymptotically stable.

Then we fix $T = 2 > T_*$, in this case the fixed points are unstable and a stable limit cycle appears (see figure 7). We observe that for bigger values of T the dynamics is qualitatively the same.

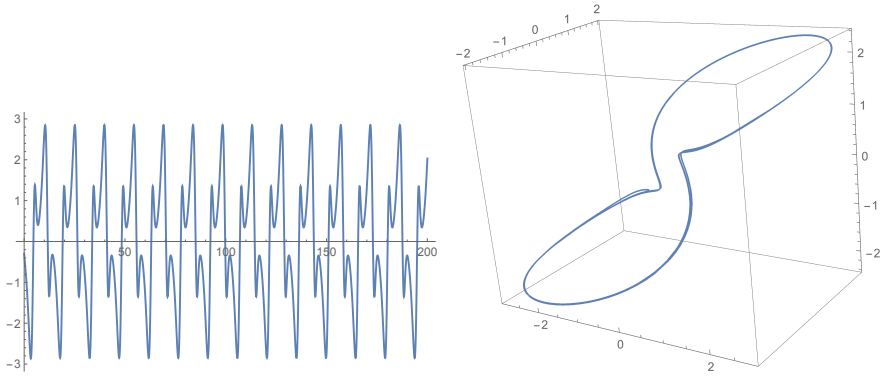

FIGURE 7. For m=2 and $T = 2 > T_*$ the fixed points $P_\pm$ are unstable and a stable limit cycle appears.

5.3. **Case $m = 3$.** Equation (21) becomes

$$\dot{x}(t) = \delta \int_{-\infty}^{t} x(r) \left(\frac{3}{T}\right)^3 \frac{(t-r)^2 e^{-\frac{3}{T}(t-r)}}{2} dr - \varepsilon \left[\int_{-\infty}^{t} x(r) \left(\frac{3}{T}\right)^3 \frac{(t-r)^2 e^{-\frac{3}{T}(t-r)}}{2} dr\right]^3. \tag{32}$$

Introducing the new variables

$$y(t) = \int_{-\infty}^{t} x(r) \left(\frac{3}{T}\right)^3 \frac{(t-r)^2 e^{-\frac{3}{T}(t-r)}}{2},$$

$$z(t) = \int_{-\infty}^{t} x(r) \left(\frac{3}{T}\right)^2 (t-r) e^{-\frac{3}{T}(t-r)} dr,$$

$$w(t) = \int_{-\infty}^{t} x(r) \left(\frac{3}{T}\right) e^{-\frac{3}{T}(t-r)} dr,$$

we rewrite equation (32) as

$$\begin{cases} \dot{x}(t) &= \delta y(t) - \varepsilon y(t)^3, \\ \dot{y}(t) &= \dfrac{3}{T}\left[z(t) - y(t)\right], \\ \dot{z}(t) &= \dfrac{3}{T}\left[w(t) - z(t)\right], \\ \dot{w}(t) &= \dfrac{3}{T}\left[x(t) - w(t)\right]. \end{cases}$$

We fix again

$$\delta = 2, \qquad \varepsilon = 1,$$

and, therefore,

$$T_* = \frac{2}{3}, \qquad P_\pm = \pm(\sqrt{2}, \sqrt{2}, \sqrt{2}).$$

We start with the value $T = 0.6 < T_*$ for which the fixed points are locally stable (see figure 8). For $T = 0.7 > T_*$ the fixed point $P_\pm$ are unstable and a stable limit

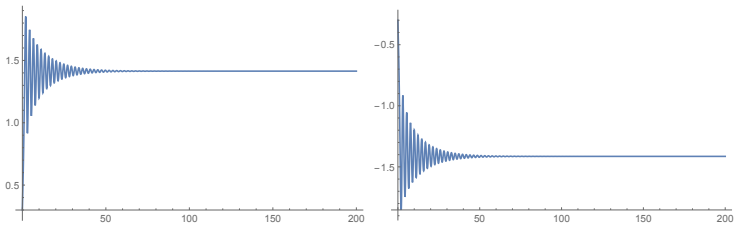

FIGURE 8. For $m = 3$ and $T = 0.6 < T_*$ the fixed points $P_\pm$ are locally asymptotically stabel

cycle appears (see figure 9). Again, as in the case with $m = 2$, the dynamics is qualitatively the same as $T > T_*$ increases.

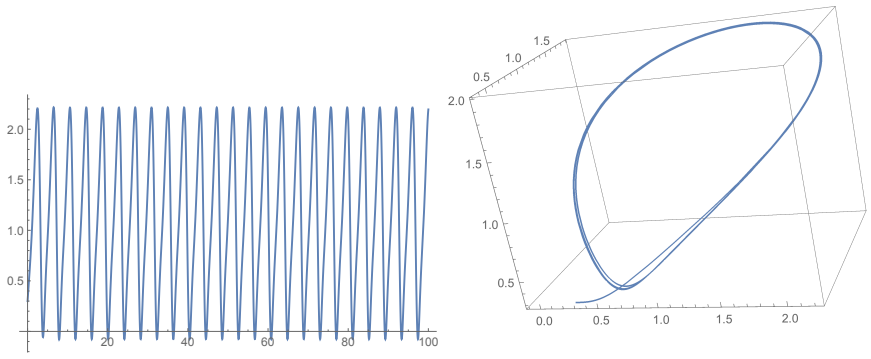

FIGURE 9. For $m = 3$ and $T = 0.7 > T_*$ the fixed points $P_\pm$ are unstable and a stable limit cycle appears.

6. **Conclusive remarks.** In this work we have considered the model introduced by Ucar in [18] with both constant and distributed delays. We have observed that the dynamics in the distributed delay case is more regular, in the sense that, as the delay parameter T is increased we have only two qualitatively different dynamical behaviour:

- the fixed points $P_\pm$ are locally asymptotically stable when the value of the parameter T is below a critical value;
- the fixed points $P_\pm$ are unstable and two stable limit cycle appears when the value of the parameter T is above a critical value.

To have a more complex dynamical behaviour we should consider more general cases. We have performed several numerical simulations to detect a more complex behaviour such as multi-periodic solutions and chaotic behaviour. For this purpose we have considered both constant and distributed delay within the same system.

6.1. **Mixed system case 1.** We consider the following equation containing a constant delay in the linear term and a distributed delay in the nonlinear one:

$$\dot{x}(t) = \delta x(t-\tau) - \left[\int_{-\infty}^{t} x(r)g(t-r)dr\right]^3, \tag{33}$$

where $g(\cdot)$ is a gamma distribution as in the previous cases. Using again the linear chain trick technique we obtain the following system for $m = 1$:

$$\begin{cases} \dot{x} = \delta x(t-\tau) - \varepsilon[y(t)]^3, \\ \dot{y} = \frac{1}{T}[x(t) - y(t)]. \end{cases} \tag{34}$$

We consider the following values for the parameters

$$\delta = 1, \qquad \varepsilon = 1.$$

Numerical simulations reveal a complex behaviour, possibly chaotic. As an example, in figure 10 we have represented the case $T = 2$ and $\tau = 5$.

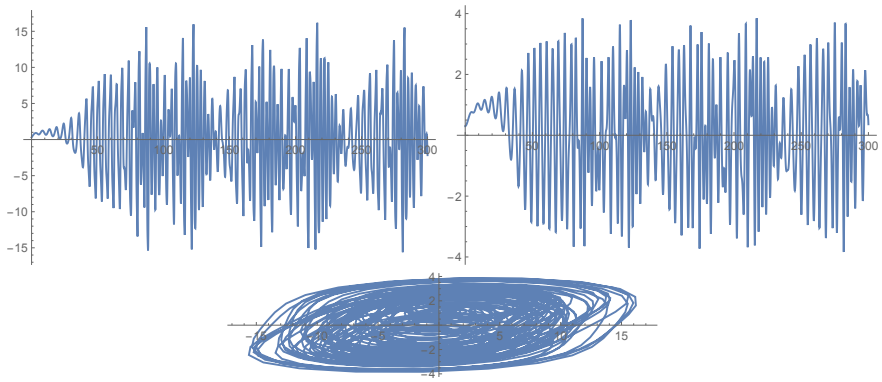

FIGURE 10. The solution of sytem (34) for $T = 2$ and $\tau = 5$. Numerical simulations suggest the evidence of a chaotic behaviour.

6.2. **Mixed system case 2.** In this second case we consider distributed delay in the linear term and constant delay in the nonlinear one:

$$\dot{x}(t) = \delta \int_{-\infty}^{t} x(r)g(t-r)dr - \varepsilon \left[x(t-\tau)\right]^3, \tag{35}$$

Using again the linear chain trick technique we obtain the following system for $m = 1$:

$$\begin{cases} \dot{x} = \delta y(t) - \varepsilon[x(t-\tau)]^3, \\ \dot{y} = \frac{1}{T}[x(t) - y(t)]. \end{cases} \tag{36}$$

In this case we set $\delta = \varepsilon = 1$ and

$$T = 1.6, \qquad \tau = 1.14.$$

Now, the dynamics appears more interesting. In figure 11 below we represent the solution where a possibly chaotic attractor appears. We note the similarity of attractor with the famous Lorenz attractor.

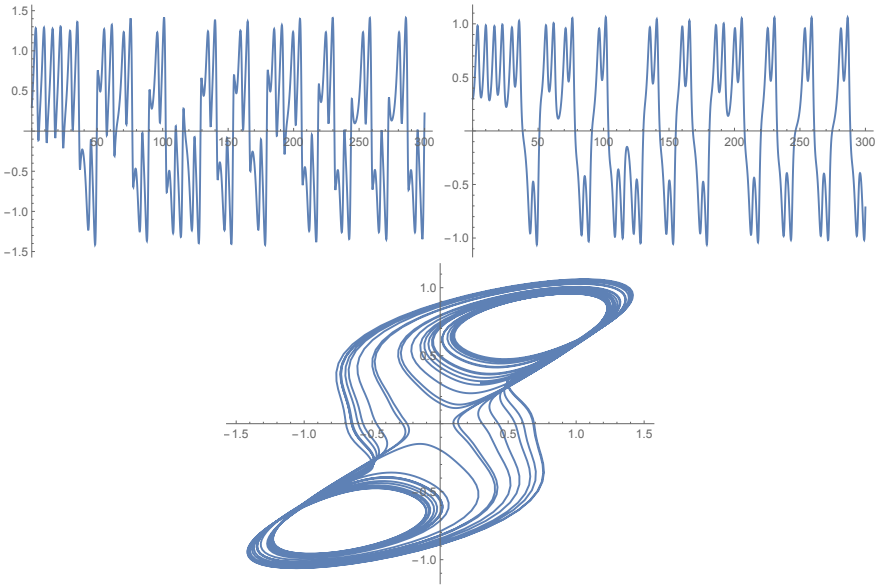

FIGURE 11. The solution of sytem (36) for $T = 1.6$ and $\tau = 1.14$. Numerical simulations suggest the evidence of a chaotic behaviour, this is supported by the presence of a strange attractor similar to the famous Lorenz attractor.

For the above simulations we consider interesting for further investigation the study of both mixed system, in particular the analysis of all possible bifurcation should be performed in the future.

Moreover, in the previous simulations we have only considered the case $m = 1$ (as done for example in [6],[7]), while in many cases (see for example [16, 15, 14]) the values of m may change the qualitative behaviour of the system. In any case, the mixed delay case (both constant and distributed) is able to recover the complex behaviour observed in the constant delay case. Of course it is interesting to wonder

wether the mixed delay case or the purely constant delay case share the same bifurcation cases or not. A more detailed analysis is needed to answer this question.

REFERENCES

[1] S. Bhalekar, Dynamics of fractional order complex Ucar system, *Studies in Computational Intelligence*, **688** (2017), 747–771.

[2] S. Bhalekar, Stability and bifurcation analysis of a generalised scalar delay differential equation, *Chaos*, **26** (2016), 084306, 7pp.

[3] S. Bhalekar, On the Ucar prototype model with incommensurate delays, *Signal, Image and Video Processing*, **8** (2014), 635–639.

[4] T. Caraballo, R. Colucci and L. Guerrini, On a predator prey model with nonlinear harvesting and distributed delay, *Comm. Pure and Appl. Anal.*, **17** (2018), 2703–2727.

[5] C. W. Eurich, A. Thiel and L. Fahse, Distributed delays stabilize ecological feedback systems, *Phys. Rev. Lett.*, **94** (2005), 158104.

[6] E. Karaoglu, E. Yilmaz and H. Merdan, Hopf bifurcation analysis of coupled two-neuron system with discrete and distributed delays, *Nonlinear Dyn*, **85** (2016), 1039–1051.

[7] E. Karaoglu, E. Yilmaz and H. Merdan, Stability and bifurcation analysis of two-neuron network with discrete and distributed delays, *Neurocomputing*, **182** (2016), 102–110.

[8] C. Li, X. Liao and J. Yu, Hopf bifurcation in a prototype delayed system, *Chaos, Solitons and Fractals*, **19** (2004), 779–787.

[9] X. Li and J. Wu, Stability of nonlinear differential systems with state-dependent delayed impulses, *Automatica*, **64** (2016), 63–69.

[10] X. Li and S. Song, Stabilization of delay systems: Delay-dependent impulsive control, *IEEE Transactions on Automatic Control*, **62** (2017), 406–411.

[11] X. Li and J. Cao, An impulsive delay inequality involving unbounded time-varying delay and applications, *IEEE Transactions on Automatic Control*, **62** (2017), 3618–3625.

[12] N. MacDonald, *Time Lags in Biological Systems*, Springer, New York, 1978.

[13] N. MacDonald, *Biological Delay Systems: Linear Stability Theory*, Cambridge University. 1989.

[14] A. Matsumoto and F. Szidarovszky, Delay dynamics in a classical IS-LM model with tax collections, *Metroeconomica*, **67** (2016), 667–697.

[15] A. Matsumoto and F. Szidarovszky, Dynamic monopoly with multiple continuously distributed time delays, *Mathematics and Computers in Simulation*, **108** (2015), 99–118.

[16] A. Matsumoto and F. Szidarovszky, Boundedly rational monopoly with single continuously distributed time delay, *Nonlinear Economic Dynamics and Financial Modelling*, Essays in Honour of Carl Chiarella, May 2014, Pages 83–107.

[17] A. H. Nayfeh, *Introduction to Perturbation Techniques*, Wiley, New York, 1981.

[18] A. Ucar, A prototype model for chaos studies, *International Journal of Engineering Science*, **40** (2001), 251–258.

[19] A. Ucar, On the chaotic behaviour of a prototype delayed dynamical system, *Chaos, Solitons and Fractals*, **16** (2003), 187–194.

Received January 2018; revised May 2018.

E-mail address: caraball@us.es
E-mail address: renatocolucci@hotmail.com
E-mail address: luca.guerrini@univpm.it